ST. ANTHONY FALLS HYDRAULIC LABORATORY
UNIVERSITY OF MINNESOTA

Project Report No. 64

LIFT AND DRAG ON SURFACE-PIERCING DIHEDRAL HYDROFOILS IN REGULAR WAVES

Submitted by
LORENZ G. STRAUB
Director

Prepared by
J. M. WETZEL and F. R. SCHIEBE

September 1960

Prepared for
David Taylor Model Basin
Department of the Navy
Washington, D.C.
under
Bureau of Ships Fundamental Hydromechanics Research Program, NS 715-102
Office of Naval Research Contract Nonr 710(32)

PREFACE

Several theoretical developments have recently been made available to predict the lift forces on hydrofoils moving through a regular seaway. The theoretical lift forces were incorporated in equations of motions in an attempt to predict successfully the longitudinal motions of a tandem hydrofoil craft. Both linear and nonlinear equations were available, as well as corrections to be applied to consider effects of unsteadiness. As few experimental data were available to verify the basic theory for a restrained system, particularly for dihedral hydrofoils piercing the surface, the current study was instigated to provide additional information.

The studies were conducted during the period of October 1, 1959, to January 31, 1960. The work was carried out under the Bureau of Ships Fundamental Hydromechanics Research Program, NS 715-102, administered by the David Taylor Model Basin, under Office of Naval Research Contract Nonr 710(32).

The entire program was under the general direction of Dr. Lorenz G. Straub, Director of the Laboratory. C. E. Bowers critically reviewed the report. John M. Killen was primarily responsible for the development of the force measuring system. Preparation of the manuscript for printing was carried out by Marjorie Summers under the general supervision of Loyal Johnson.

A B S T R A C T

Experimental measurements were made of the lift and drag of a restrained surface-piercing dihedral hydrofoil in regular head and following seas. Two velocities and a variety of wave lengths and amplitudes were used. The oscillatory lift was predicted with fair success using linearized theory as developed by Ogilvie. The experimental forces were observed to contain harmonic distortion, and comparison of the second harmonic component obtained from nonlinear quasi-steady theory indicated that the calculated values were too low. No theory was available for comparison with the oscillatory drag forces.

Tests with a restrained tandem dihedral configuration in smooth water indicated that the performance ratio of the aft foil could be considerably increased for a particular separation of the foils. The optimum separation increased with increasing velocity. A brief series of tests were made in head seas using the optimum foil separation, and little difference between the tandem foils and single foil was noted for the oscillatory lift component.

C O N T E N T S

	Page
Preface	iii
Abstract	iv
List of Illustrations	vi
List of Symbols	vii
I. INTRODUCTION	1
II. THEORETICAL CONSIDERATIONS	2
III. EXPERIMENTAL APPARATUS	6
A. Test Facility	6
B. Dynamometer and Apparatus	7
C. Procedure	8
D. Data Reduction	9
IV. DISCUSSION OF RESULTS	9
A. Steady Forces	9
B. Oscillatory Lift Forces	10
C. Oscillatory Drag	11
D. Tandem Interference Tests in Smooth Water	12
E. Tandem Interference Tests in Rough Water	13
V. CONCLUSIONS	14
List of References	15
Figures 1 through 15	19
Appendix	37
Distribution List	43

LIST OF ILLUSTRATIONS

Figure		Page
1	Definition Sketch.	19
2	Effect of Unsteadiness on Forces	20
3	Sketch of Dynamometer and Apparatus.	21
4	Force Coefficients for Smooth Water.	22
5	Oscillatory Lift Forces and Phase Relationships, Head Seas . .	23
6	Oscillatory Lift Forces and Phase Relationships, Head Seas . .	24
7	Oscillatory Lift Forces and Phase Relationships, Following Seas	25
8	Comparison of Nonlinear Theory and Experimental Lift	26
9	Percentage of Second Harmonic Distortion in Lift	27
10	Oscillatory Drag Forces and Phase Relationships, Head Seas . .	28
11	Oscillatory Drag Forces and Phase Relationships, Following Seas	29
12	Lift Coefficients for Aft Foil of Tandem Configuration in Smooth Water	30
13	Drag Coefficients for Aft Foil of Tandem Configuration in Smooth Water	31
14	Performance Ratio for Aft Foil of Tandem Configuration	32
15	Oscillatory Lift Forces for Aft Foil of Tandem Configuration in Head Seas	33

LIST OF SYMBOLS

A - Mean value of exponential decay of orbital velocity over depth of foil.

a - Wave amplitude.

b - Foil chord.

C - Theodorsen function.

C_D - Drag coefficient.

C_L - Lift coefficient.

c - Wave celerity.

c_o - Smooth water lift coefficient.

c' - Lift curve slope.

D_m - Maximum amplitude of oscillatory drag.

d - Submergence of foil apex.

E - Unsteady force correction factor.

i - $\sqrt{-1}$

J_o - Bessel function of 1st kind, order zero.

J_1 - Bessel function of 1st kind, order one.

k - Wave number, $2\pi/\lambda$.

L - Lift.

L_m - Maximum amplitude of oscillatory lift.

L_w - Amplitude of oscillatory lift.

t - Time.

V - Velocity.

α - Angle of attack.

ρ - Fluid density.

λ - Wave length.

μ - Dihedral angle.

ν - Frequency of encounter $2\pi/\lambda.(V \pm c)$.

ϕ - Phase angle of oscillatory lift.

ω - Circular frequency.

Numerical subscripts on forces indicate order of harmonics; subscripts f and a indicate forward or aft foil.

LIFT AND DRAG OF SURFACE-PIERCING DIHEDRAL HYDROFOILS IN REGULAR WAVES

I. INTRODUCTION

Early investigations of hydrofoils were concerned with determination of the forces acting on standard airfoil sections in smooth water. Two basic foil systems were considered: completely submerged flat foils and dihedral or surface-piercing foils. To date most work has been done with the former perhaps due to the relative ease in theoretical formulation. However, recent theoretical work has also been stimulated for the dihedral surface-piercing hydrofoil. At the present time, several theories are thus available that predict the lift forces of both types of hydrofoils moving through either smooth water or regular seas. The knowledge of such forces is basic if an accurate prediction of the motion of a hydrofoil craft is to be attained. In actual application, the issue is somewhat complicated by the fact that tandem foil systems are necessary to achieve the desired longitudinal stability. Certain assumptions must then be made and verified regarding the interference effect of one foil on another. Some experiments concerning longitudinal motions of a tandem dihedral-foil craft are described in Reference [1].*

As a hydrofoil passes through waves, oscillatory forces are experienced by the foil. This results in an unsteady flow pattern being developed, and attempts have been made to include the effects of unsteadiness by utilizing available unsteady airfoil theory. In most cases, adequate experimental verification of the forces is not available.

This report describes results of tests conducted with dihedral surface-piercing hydrofoils. Lift and drag measurements were made in smooth water and in regular head and following seas. Some brief tests were also made to determine the influence of the forward foil on the forces of the rear foil in a tandem arrangement of foils. The contract was supported by the David Taylor Model Basin, under terms of Contract Nonr 710(32).

---

*Numbers in brackets refer to List of References on p. 15.

II. THEORETICAL CONSIDERATIONS

Several investigators have developed theories for the lift of a hydrofoil in smooth water and regular seas. The theories have then been extended to be applicable in the prediction of the longitudinal stability and motions of a hydrofoil craft. Perhaps the most useful of these theories have been proposed by Kaplan [2] and Ogilvie [3]. In both cases, the effects of unsteadiness have also been considered. In its present form, the theory by Kaplan applies to flat foils of finite span in a tandem configuration. He also includes the effect of the downwash of the forward foil on the rear foil. Ogilvie developed his theory for a surface-piercing foil, and thus it proved to be the most useful in the current program. A brief summary of the pertinent equations will be presented in this report.

As a surface-piercing hydrofoil restrained in motion moves through rough water, the lift force will oscillate about some steady value. This oscillation, as a rough approximation, will be caused by two effects. The angle of attack will be changed by the vertical component of the orbital velocity, and the area of the foil will be changed by the fluctuating water surface. This is schematically shown in Fig. 1 for the foil moving against oncoming sinusoidal waves, i.e., head seas. The orbital velocity of a particle at the surface is shown at several points of the wave. The maximum vertical velocity occurs at the midpoint between the crest and trough of the wave. In the case shown, the instantaneous angle of attack (the ratio of the vertical component of orbital velocity to foil velocity) decreases on the downward slope of the wave and increases on the upward slope. This will, of course, cause a corresponding change in lift at these particular locations, and the conditions will be favorable for following the wave profile. If we now consider the case of following seas with the foil moving in the same direction as the wave, it will be noted that the situation is reversed. As the foil approaches the downward slope of the wave the angle of attack is increased, resulting in an increase in lift. As the foil moves through the trough towards the crest, the angle of attack is decreased just at the point where an increase in lift would be desirable to carry the craft over the crest. This unfavorable effect is reduced with increasing velocity of the foil, since the change in angle of attack is then reduced.

The broken circles represent the exponential decay of the orbital velocity with depth. It is thus seen that the instantaneous angle of attack, which is directly dependent on the vertical component of orbital velocity, continually changes along the span of a dihedral foil. In analysis, an average value will be taken as seen in later developments.

In general, the following assumptions were made for a restrained dihedral foil moving through regular waves:

(1) The lift curve slope is a constant,

(2) Waves generated by the forward foil are neglected, and

(3) Effect of the free surface is negligible.

The effect of downwash from the forward foil was also neglected, but later investigation indicated that this assumption was reasonable.

To simplify formulation, expressions were first derived assuming quasi-steady conditions. The restriction of a quasi-steady flow implies that the lift at any instant is the same as it would be in smooth water at the same instantaneous angle of attack and submergence. Thus, the effects of unsteadiness are not considered. The lift on the foil is then defined as

$$L = 1/2\ \rho\ AV^2\ [c_o + c'\alpha]$$

The nonlinear quasi-steady expression for the lift on a restrained foil is given by

$$L = \rho\, bV^2\ \cot\mu\,[d + a\cos\nu t]\ \left\{c_o \mp \frac{c'}{V}\, a\omega A \sin\nu t\right\} \qquad (1)$$

or after expanding and considering only the oscillatory part of the lift due to the action of the waves,

$$L_w = a\ \rho\ bV^2\ \cot\ \mu\left\{\sqrt{c_o^2 + \left(\frac{c'd\omega A}{V}\right)^2}\ \cos\ (\nu t - \phi_1) \mp \frac{c'a\omega A}{2V}\ \sin 2\nu t\right\} \qquad (2)$$

where a = wave amplitude,

ρ = fluid density,

b = foil chord,

μ = dihedral angle,

c_o = smooth water lift coefficient,
c' = lift curve slope,
d = submergence of apex of foil,
ω = circular frequency,
A = mean value of exponential decay of orbital velocity over depth of foil,
ν = frequency of encounter, $2\pi/\lambda\ (V \pm c)$,
c = wave celerity,
λ = wave length, and
$\phi_1 = \tan^{-1} \mp \frac{c'd\omega A}{Vc_o}$ phase of fundamental.

In either of these equations, the upper sign is to be taken with head seas, and the lower sign with following seas. As the orbital velocity varies with depth, an average value is taken over the depth of submergence of the foil. The term A accounts for the exponential decay of the orbital velocity with distance from the free surface. From Eq. (2) it will be noted that a second harmonic component is present that varies directly with wave amplitude. The values of c_o and c' may either be determined experimentally or obtained from theory such as developed by Wadlin [4]. The magnitude of c_o will be small in comparison with c', and the second term under the radical in Eq. (2) will be much greater than the first term, unless very high speeds are considered. Thus, for these conditions, if one writes a ratio of the amplitude of the second term to the first term, the harmonic distortion is practically independent of the wave length. In fact, it will be noted that the oscillatory lift is very sensitive to the lift curve slope c'. However, the phase relationship between the wave and the lift is affected significantly by the smooth water lift coefficient.

The linearized quasi-steady equation is obtained by considering only small values of the wave amplitude, thereby permitting the terms containing second and higher powers of the amplitude to be neglected. The phase of the fundamental is of course not affected by linearization. By neglecting the nonlinear term, the oscillatory lift no longer depends on the direction of motion with respect to the waves, i.e., head or following seas. The phase angle will still maintain this dependency, however.

Ogilvie determined the unsteady effects by making an analogy with a similar problem in aerodynamics and using the results obtained for this case.

It was necessary at this time to additionally assume that the three-dimensional foil behaves similarly to the two-dimensional wing in this respect. Two types of unsteadiness were considered for the restrained system: that arising from the unsteady wake vorticity due to the change in circulation about the foil and the nonuniformity of the velocity over the chord. The latter is of significance when the foil chord length is not small compared to the wave length. Only the linearized system was considered to determine the effects of unsteadiness. The following expression for the oscillatory lift was found by using Ogilvie's equations with the heave and pitch set equal to zero (restrained system).

$$L = R_e \left[\mp i\rho\, bV^2 \cot\mu \frac{a\omega c' dA}{V} \left\{ \left[J_o\ (kb/2) - iJ_1\ (kb/2) \right] C\left(\frac{\nu b}{2V}\right) \right.\right.$$

$$\left.\left. + i\,(1 \mp c/V)\, J_1\ (kb/2) \right\}\ e^{i\nu t} + \rho\, bV^2 \cot\mu\ c_o\ a e^{i\nu t} \right] \qquad (3)$$

where the variables are the same as previously defined. The new symbols introduced are:

k = wave number, $2\pi/\lambda$,
C = Theodorsen function with argument $\nu b/2V$, and
J_o, J_1 = Bessel function of first kind, orders zero and one respectively.

The terms in braces represent the unsteadiness correction factor. For the quasi-steady case, this complex quantity will take on the value of unity. Equation (3) will then be identical to the one obtained by linearizing Eq. (2).

The reduced frequency, $\nu b/2V$, is a useful measure of the unsteadiness effects. Unsteadiness will be most important for large values of $\nu b/2V$. The arguments of the Bessel functions can be related to the reduced frequency by the relation

$$\frac{kb}{2} = \frac{\nu b}{2V}\left[\frac{1}{1 \mp \frac{c}{V}}\right] \qquad (4)$$

It will be noted that the arguments are then a function of the velocity as well as the reduced frequency. A polar plot of the effects of

unsteadiness on the lift forces is shown in Fig. 2 for the ranges of interest of the current studies.

In the case of the dihedral surface-piercing foil, another source of unsteadiness arises that has no counterpart in aerodynamic theory. This is associated with the variation of span as the foil moves through a wave train. Based on previous work considering unsteady effects of a flat foil near the free surface, it was felt that the complexity of analysis would prevent an adequate solution for the dihedral foil and was thus dismissed from further consideration at the present time.

Little theoretical work is available concerning the interference effects of two dihedral foils placed in tandem. A theory developed by Nishiyama [5] for flat foils in smooth water indicates that for given conditions an optimum spacing of the foils exists that will provide the best performance ratio (lift/drag). The improvement is obtained by placing the rear foil in the maximum upwash of the stationary wave (with respect to the foil) generated by the forward foil. No adequate experimental verification of this effect has been found. Nishiyama has also developed a general theory for dihedral hydrofoils [6] that can be extended to describe the pattern of the surface disturbance behind the foil. The expression is somewhat complicated, and will not be further described here, although the computations should be carried out to be used in conjunction with the experimental data presented in this report. The effect of the downwash of the dihedral foil is also not completely understood, particularly with regard to the decay of the vorticity with increasing disturbance from the forward foil.

III. EXPERIMENTAL APPARATUS

A. Test Facility

The tests were run in the multi-purpose test channel which is 9 ft wide, 6 ft deep, and 220 ft long. The water depth was maintained at 4.5 ft for all tests with a resulting critical velocity of about 12 fps. The channel is equipped with a towing carriage and a wave generator. The towing carriage is self-propelled with two 5 hp D.C. motors whose rpm is precisely controlled by a Thy-mo-trol system. Carefully regulated speeds up to a maximum of 25 ft/sec are available in either direction. The wave generator is of the hinged plate type, and is capable of generating waves from slightly less than

3 ft to 40 ft in length with various amplitudes. The largest wave that can be generated is about 16 ft long and 2 ft high. A permeable beach sloping absorber is located at the far end of the channel to minimize reflections. A more complete description of the test facility can be found in Reference [7].

B. Dynamometer and Apparatus

To satisfactorily measure the oscillatory forces on the foils, considerable attention was given to the development of a suitable dynamometer. A two component system (lift and drag) was constructed from two parallel aluminum plates 1/4 in. thick which were held to a 1/2-in. spacing by four flexures (1/2 x 0.020) at each corner. A strain element, 1/2 x 0.001-in. steel shim stock, was positioned between the plates so as to be in direct tension as a result of any parallel motion of one plate with respect to the other.

Two to four strain gages are mounted on the shim stock for force measurement.

An adjusting screw permits pretensioning the strain element so that both negative and positive forces may be measured. A schematic drawing of this dynamometer is shown in Fig. 3.

The proposed advantages of this system are:

(1) Small displacement ($\approx 800\mu$ in. full scale),

(2) High natural frequency, and

(3) Small response to normal forces.

Normal force response should be small because of the smaller deflection of the mechanical system from normal forces than from parallel forces. For this to be a minimum, the flexures should be as nearly perpendicular to the plates as possible and the plates should be very nearly parallel. Any bending of the baseplates should be partly canceled by the differential connection of the strain gages.

Two units are assembled with their force measuring axes at right angles to form the dynamometer assembly.

As the drag component was required to be considerably more sensitive than the lift, it was found that carriage vibration created a rather serious

problem. In an effort to reduce this vibration, the dynamometer was mounted on a large steel beam that was suspended from the towing carriage by means of flexible supports as shown in Fig. 3. The beam was also restricted in surge, and measurements of the motion of the beam under actual test conditions indicated very little movement.

Two identical aluminum foils with a Wright 1903 section were available for the tests. The foils had a 45 degree dihedral angle and a 2-in. chord. These foils were the same as those used in the stability tests described in Reference [1]. Some brief tests were also made with a NACA 0012 section with a 45 degree dihedral angle and 2-in. chord.

The signals from the dynamometer were amplified and recorded with a Sanborn 4-channel recorder system. The wave profile was measured with a sonic wave transducer attached to the carriage. The sonic head was mounted directly across from the quarter chord point of the foil to reduce the calculations in phase determinations. A complete description of the sonic transducer is given in Reference [8].

C. Procedure

Measurements were made of the lift, drag, wave profile, and carriage speed. Velocities of 5, 8, and 10 fps were used for most tests, although few data were taken in following seas at 5 fps. For the latter case, wave lengths were limited to those for which the wave celerity was less than the towing speed. Velocities of 10 fps were restricted to the NACA 0012 foil due to structural problems associated with the Wright 1903 section. Wave lengths of 3 to 8 ft were used with wave amplitudes varying from about 0.05 to 0.2 ft. The higher amplitudes were not used for the shorter wave lengths, as the generated waves were not stable over the test length under these conditions.

First tests were made in smooth water to determine the steady force characteristics for the particular foil geometry. The lift coefficients and lift curve slope were required for the theoretical analysis. The foil was set at a submergence of 6 in. and an angle of attack that would provide a lift coefficient similar to the value used in the previous tests with the tandem craft as described in Reference [1]. Force measurements then were made in both head and following seas. No ventilation of the foils was observed for any of the wave conditions or towing speeds utilized in the investigation.

Tests were also made with a restrained tandem configuration utilizing identical foils with the Wright 1903 section. The forward foil was placed directly in line longitudinally with the rear foil and at the same submergence. The rear foil was attached to the dynamometer to permit determination of the lift and drag forces. The fore and aft separation of the two foils was adjusted by moving the forward foil. Brief tests were also made with the optimum foil separations in head seas.

D. Data Reduction

Examination of the experimental records indicated that higher harmonics were also being obtained. To determine the amount of harmonic distortion in the recorded data and to obtain a better basis for determining phase relationships, a harmonic analysis was made of most of the records. A graphical method was used that is described in Reference [9]. Only the fundamental and second harmonic component have been plotted; the higher harmonics are tabulated in the Appendix for the lift and drag forces.

IV. DISCUSSION OF RESULTS

A. Steady Forces

Measurements were made of the forces on the foils in smooth water to establish values of the lift coefficient and lift-curve slope as required in the theoretical determination of the oscillatory forces. Under other conditions, these values could also have been obtained from theoretical work such as that proposed by Wadlin [4]. For purposes of these tests, which was to verify the oscillatory forces, it was desired to use the experimental values. The force coefficients are plotted as a function of angle of attack in Fig. 4. The area of the dihedral foil was taken to be the projected area on a horizontal plane. A comparison of data for the Wright 1903 section with that taken from Reference [10] is shown in Fig. 4 with good agreement being observed. The accuracy of the drag data is not as good as the lift, due to difficulties experienced with carriage vibration. However, the data are included to provide an order of magnitude for future comparisons. The increase in drag with lower velocity is probably caused by the higher wave drag at this velocity, as has been substantiated by others.

Some data were also taken with another airfoil section, the NACA 0012, which is a symmetrical profile. The lift and drag coefficients are shown in Figs. 4c and d. As the section was symmetrical, the angle for zero lift should be approximately zero. In any case, the lift-curve slope is of most interest, and this is independent of the angle of attack up to the stall point of the foil. The lift coefficient itself is also of more interest for this program than the angle of attack associated with the lift coefficient, as can be seen from the theoretical equations.

B. Oscillatory Lift Forces

The oscillatory lift force has been plotted in terms of a dimensionless parameter. This parameter was obtained from Eq. (2) or (3) and contains the wave amplitude. Thus, if nonlinearity due to large wave amplitudes is negligible, the data plotted in this manner should be independent of the amplitude. Figures 5, 6, and 7 show data for the two towing velocities and head or following seas. Only the linearized theoretical curves are plotted for the quasi-steady and unsteady cases. The oscillatory lift, L_{m_1}, has been taken as the maximum amplitude of the first harmonic as determined from the harmonic analysis of the experimental record. The subscript denotes the order of the harmonic, the number one referring to the fundamental. The data agree with the theory fairly well, with the exception of the longer wave lengths in head seas. The measured lift appears to be somewhat higher than predicted by either theory, particularly at the higher velocity. For following seas, Fig. 7, the data lie slightly below the theoretical curves. Phase relationships seem to be within about 10 to 20 degrees of the predicted values. Some of the scatter of the data exists from the fact that various wave amplitudes were used. For the oscillatory lift, no definite trend could be found with amplitude. It will also be noted in comparing Figs. 5 and 6 that unsteady effects are decreased in head seas with increasing velocity for the same range of wave conditions. This is related to the decreasing value of the reduced frequency of encounter.

In conjunction with the measurements of the oscillatory forces for the lower velocity, in several instances a burst of oscillation would occur at the same position (near the wave trough) with respect to the wave profile. This oscillation was of rather high frequency as compared to the frequency of encounter, and of relatively short duration.

A comparison has also been made with the quasi-steady, nonlinear theory given by Eq. (2). This comparison is shown in Fig. 8 for typical cases in head and following seas. Again it will be seen that the experimental data lie slightly above the theoretical curve for head seas, the opposite being true for following seas. Both the experimental and theoretical responses are seen to contain some distortion. Results of the harmonic analysis of the lift data are shown in Fig. 9. The second harmonic distortion in the experimental records was considerably larger than predicted. As mentioned in an earlier section, the ratio of the amplitudes of the nonlinear term to the fundamental results in a factor that does not depend greatly on the wave length. This is true for the described test conditions where c_o is small in comparison with c' and the foil moved through the rough water at rather low speeds. For this reason, only one theoretical curve has been shown for the ranges of wave lengths encountered. The discrepancy between the theory and experiment led to an investigation of the wave profile used as the forcing function in the experiments. A harmonic analysis was made of several typical wave forms and a distortion of about 8 to 12 per cent was found in most cases. It would be interesting as well as desirable to use the actual wave profile in the theory to determine the effect on the lift force.

Limited data were taken with the NACA 0012 section. The experimental records of the oscillatory forces, particularly the drag, were difficult to analyze. The natural frequency of the system was sufficiently lowered due to the greater weight of this foil to cause additional problems. The oscillatory lift data are tabulated in the Appendix along with theoretical values for the quasi-steady and unsteady linearized lift. No harmonic analysis was made for these records; therefore, the values listed represent peak-to-peak measurements measured directly from the records rather than the maximum amplitude of the fundamental. Oscillatory drag forces and phase relationships are not reported as the records would not permit the determination of these quantities with sufficient accuracy.

C. Oscillatory Drag

No theory is known at the present time to predict the drag forces for a foil moving through waves. The experimental data for the Wright 1903 section are plotted in Figs. 10 and 11. A dimensionless parameter similar to the one used for lift has been arbitrarily adopted. This parameter has shown

little dependence on wave length and is thus plotted as a function of wave height (peak-to-peak) in these figures. The raw data are tabulated in the Appendix.

The records for the drag forces indicated considerably more harmonic distortion than for the lift. Harmonic analysis was made of the records and only the amplitude of the fundamental was plotted in these figures. The results of the harmonic analysis indicating the percentage of higher harmonic content are also given in the Appendix. The drag data are plotted on a smaller scale, as the accuracy of the measurements is considerably less than for the lift. The vibration of the carriage created some difficulty in reading the records accurately and, although attempts were made to eliminate the surge of the supporting beam without transmitting carriage vibration, these attempts were not completely successful. It is felt that such surge may have been partially responsible for some of the higher harmonics that appeared in the experimental drag.

D. Tandem Interference Tests in Smooth Water

The Wright 1903 hydrofoil used in all preceding tests was combined with another of similar geometry in a tandem configuration. Each of these foils was placed at a given angle of attack, two particular values being used for the forward foil. The forward foil was attached to a device that could be moved in the longitudinal direction to vary the separation of the foils. The rear foil was attached to the dynamometer. As the distance between the foils was changed, the forces on the rear foil also were changed. Typical results are shown in Figs. 12 and 13 for lift and drag. The two sets of data points for each velocity represent different angles of attack or their corresponding lift coefficients of the forward foil. The force coefficients for one foil alone (infinite separation) are also shown. The effect of velocity can be seen to move the location of the maximum forces. In both cases it seems that the interference effect is practically negligible at foil separations of about 30 chords or more.

In comparing Figs. 12 and 13, it will be noted that the lift and drag are out of phase, the maximum values being obtained at different foil separations. For certain spacings of the two foils it is possible to increase the lift over the value for the one foil alone, whereas the drag may be decreased. To present a useful arrangement of data, a plot of performance ratio

or ratio of lift to drag is shown in Fig. 14 for the two available towing velocities. The performance ratio for the rear foil alone is about 11 and 12 for the velocities of 5 and 8 fps, respectively. Data are shown for two lift coefficients for the forward foil. As the lift on the forward foil is reduced, the changes in the performance ratio of the rear foil are not as great although the same general trend is observed. For the larger lift coefficient of the forward foil, the performance ratio is roughly twice that for a single foil alone. The foil separation at which this maximum occurs depends on the velocity. The optimum separation increases with increasing velocity as can be seen in Fig. 14. Actually, a considerable range of separations exists that will still provide an effective increase in the performance ratio of the aft foil.

E. Tandem Interference Tests in Rough Water

Some brief tests were made with the previous tandem configurations in regular head seas. Both foils were restrained, and the forward foil was set to provide a lift coefficient of 0.67, one of the same values used for the smooth water tests. Two foil separations were used. Separations of 10 and 18 chords were selected as these gave the maximum performance ratio as determined from Fig. 14. The results for three wave lengths are shown in Fig. 15. No harmonic analysis was made for the experimental responses. The theoretical curves were calculated by previous equations which neglected the influence of the forward foil. The wave amplitude for these tests was nominally about 0.1 ft. In comparing the results of the tandem foils in waves with those of Figs. 4 and 5 for a single foil, it will be noted that little difference actually exists. The oscillatory lift for the higher velocity appears to be somewhat lower at the longer wave lengths than that found for the single foil. The relative insignificance of the interference effect of the tandem foils under these conditions may be somewhat expected. For the particular foil separations used, it will be noted that the smooth water lift coefficient for the aft foil of the tandem configuration is considerably higher than for the aft foil alone. For the velocities used in these tests, the smooth water lift coefficient does not have much effect on the oscillatory lift parameter, as the magnitude of the term containing the lift-curve slope is much greater and thus is essentially the controlling factor. However, as the lift on the forward foil is continually changing, the associated wave train would also be

affected. Therefore, unsteadiness effects could possibly result in some differences for other wave conditions. More work on the interference effect of the tandem foil configurations is currently being anticipated in conjunction with another hydrofoil program.

V. CONCLUSIONS

Based on the experimental data for restrained dihedral foils and range of conditions utilized in the investigation, it is possible to make the following conclusions:

(1) In general, the linearized theory reduced from Ogilvie's equations of motion for a restrained dihedral foil in regular head and following seas gave qualitative agreement with experimental data of oscillatory lift. The consideration of unsteadiness in some cases slightly improved the correlation.

(2) The amplitude of the second harmonic of the oscillatory lift as predicted by quasi-steady theory was smaller than the experimental as determined by harmonic analysis.

(3) An interference effect existed between identical forward and aft foils in smooth water for foil separations less than 30 chords. For a foil separation of 10 or 18 chords and velocities of 5 and 8 fps respectively, it was possible to increase the performance ratio of the aft foil by about a factor of 2.

(4) Brief tests indicated little interference effect with tandem foils in head seas.

LIST OF REFERENCES

[1] Wetzel, J. M. Experimental and Analytical Studies of the Longitudinal Motions of a Tandem Dihedral Hydrofoil Craft in Regular Waves. University of Minnesota, St. Anthony Falls Hydraulic Laboratory Technical Paper No. 30, Series B, April 1960.

[2] Kaplan, Paul. Longitudinal Stability and Motions of a Tandem Hydrofoil System in a Regular Seaway. Stevens Institute of Technology, Davidson Laboratory Report No. 517, December 1959.

[3] Ogilvie, T. Francis. The Theoretical Prediction of the Longitudinal Motions of Hydrofoil Craft. David Taylor Model Basin Report 1138, November 1958.

[4] Wadlin, Kenneth L. and Christopher, Kenneth W. A Method for Calculation of Hydrodynamic Lift for Submerged and Planing Rectangular Lifting Surfaces. National Advisory Committee for Aeronautics Technical Note 4168, January 1958, 34 pp.

[5] Nishiyama, Tetsuo. "Hydrodynamic Investigation on the Submerged Hydrofoil, Part III," American Society of Naval Engineers Journal, February 1959, pp. 135-142.

[6] Nishiyama, Tetsuo. "Lifting-Line Theory of the Submerged Hydrofoil of Finite Span, Part II, Hydrodynamic Characteristics of the Submerged Hydrofoil of Dihedral Angle," American Society of Naval Engineers Journal, November 1959, pp. 693-700.

[7] Straub, L. G. and Bowers, C. E. The St. Anthony Falls Multi-Purpose Test Channel. University of Minnesota, St. Anthony Falls Hydraulic Laboratory Technical Paper No. 17, Series B, July 1956.

[8] Killen, J. M. The Sonic Surface-Wave Transducer. University of Minnesota, St. Anthony Falls Hydraulic Laboratory Technical Paper No. 23, Series B, July 1959.

[9] Anonymous. Reference Data for Radio Engineers, 3rd Edition. International Telephone and Telegraph Corporation, New York, New York, 1949.

[10] Leehey, Patrick and Steele, John M. Jr. Experimental and Theoretical Studies of Hydrofoil Configurations in Regular Waves. David Taylor Model Basin Report 1140, October 1957.

F I G U R E S

(1 through 15)

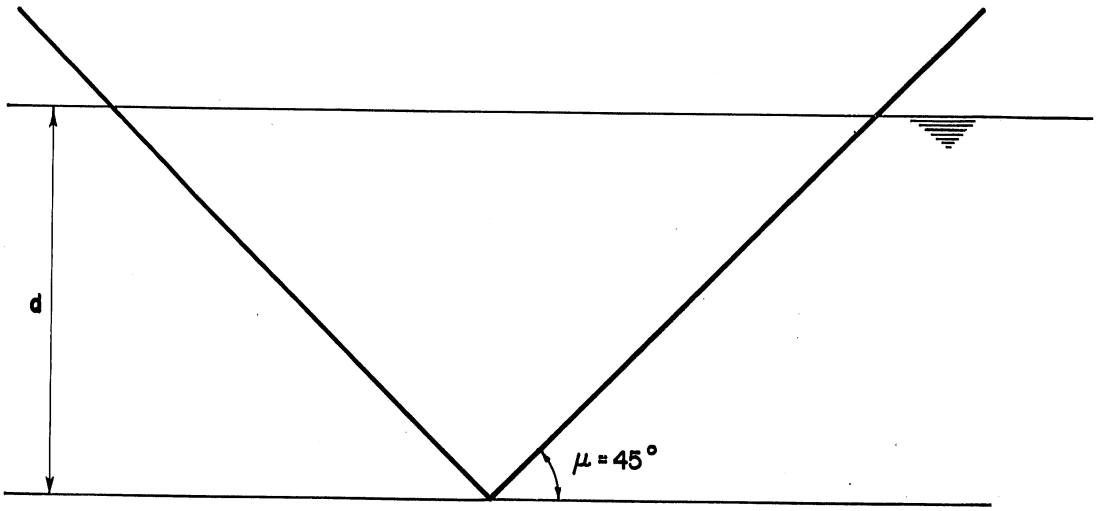

Smooth Water

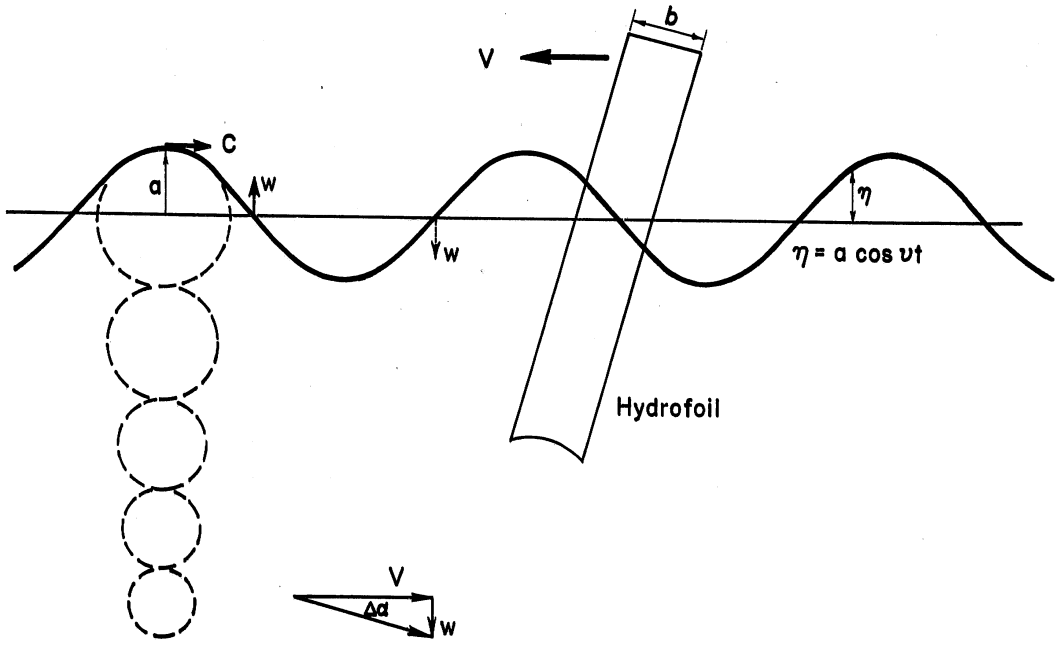

Rough Water

Fig. 1 - Definition Sketch

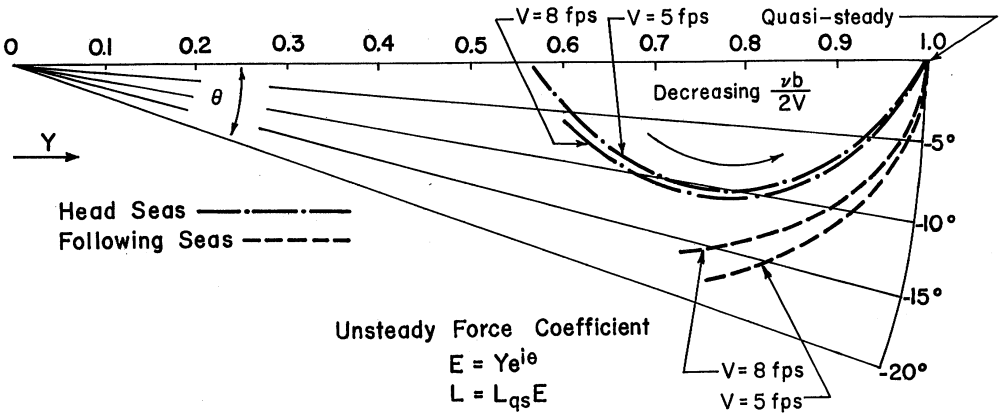

Fig. 2 – Effect of Unsteadiness on Forces

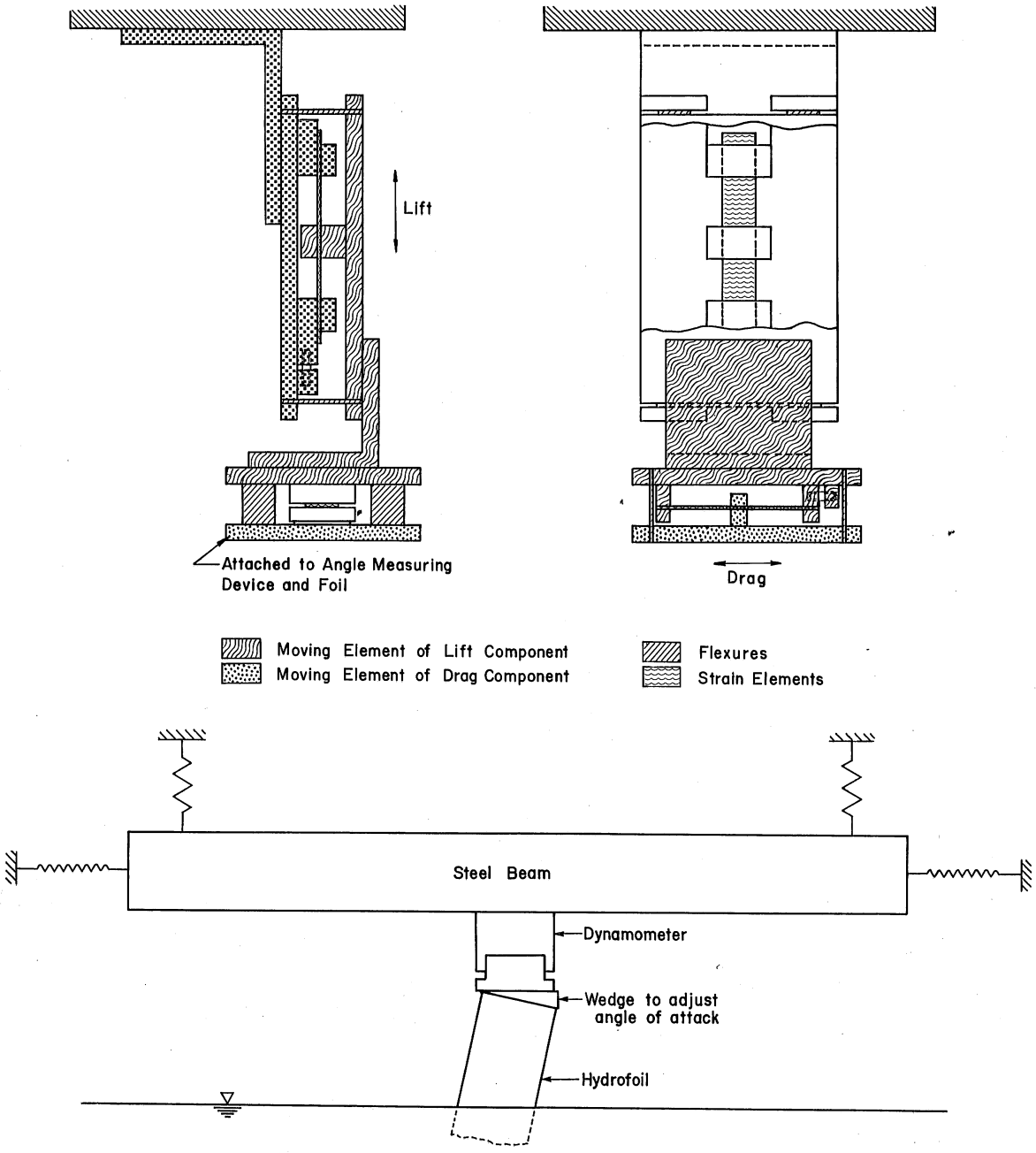

Fig. 3 – Sketch of Dynamometer and Apparatus

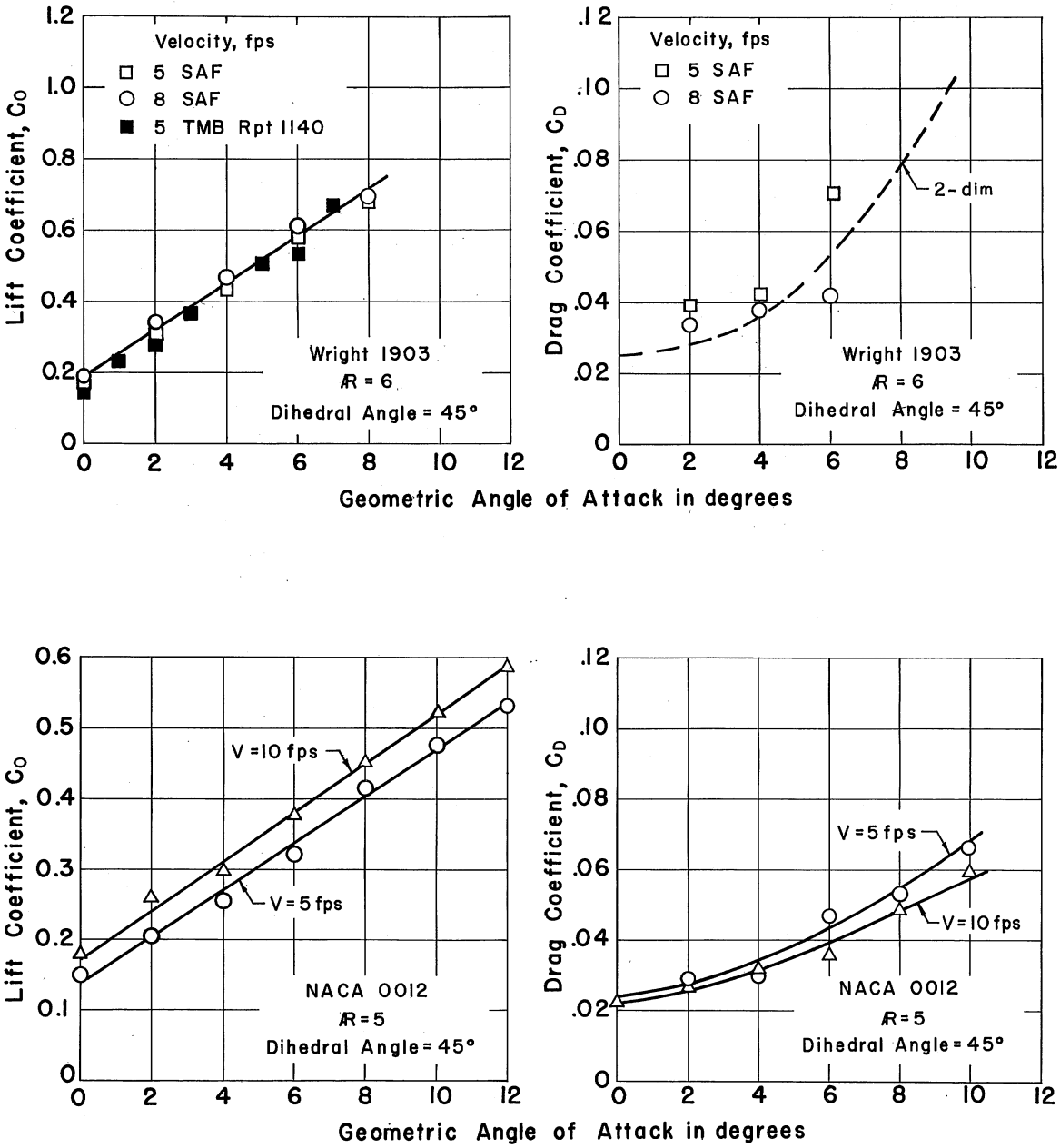

Fig. 4 – Force Coefficients for Smooth Water

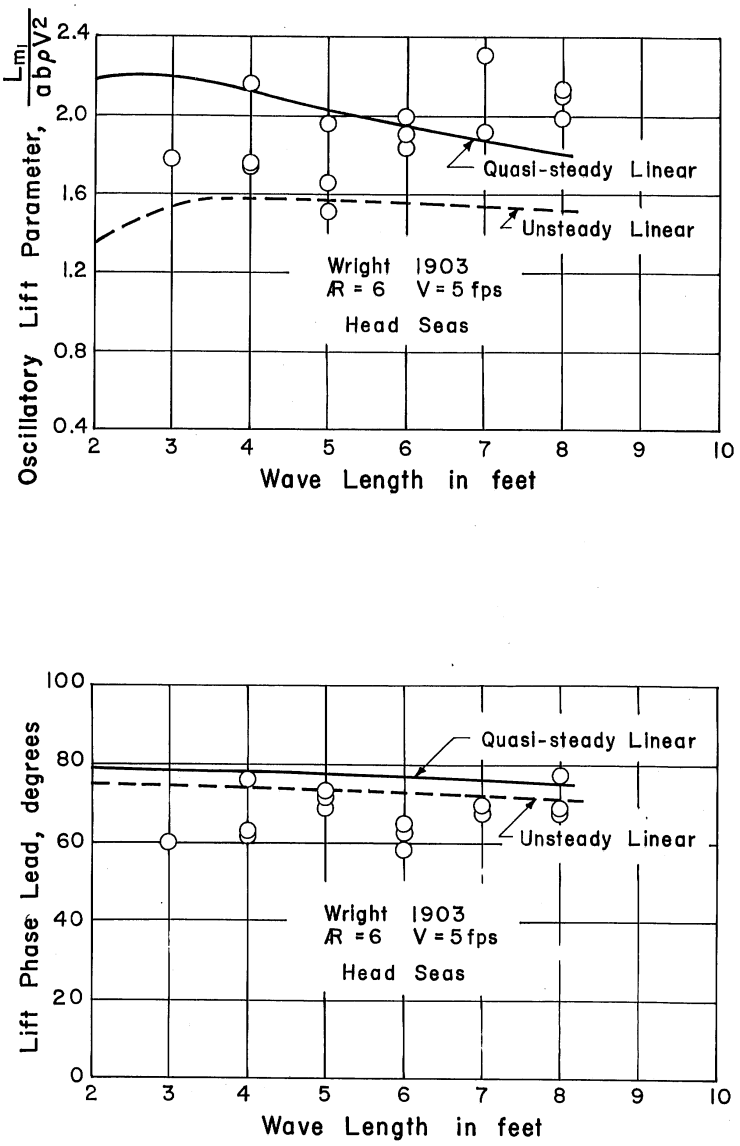

Fig. 5 - Oscillatory Lift Forces and Phase Relationships, Head Seas

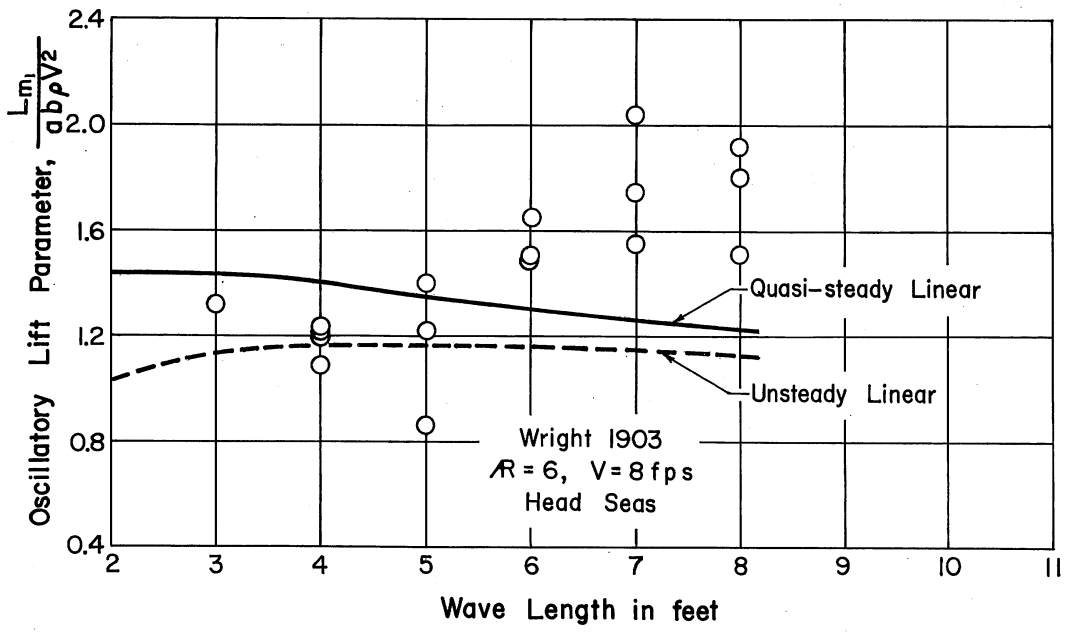

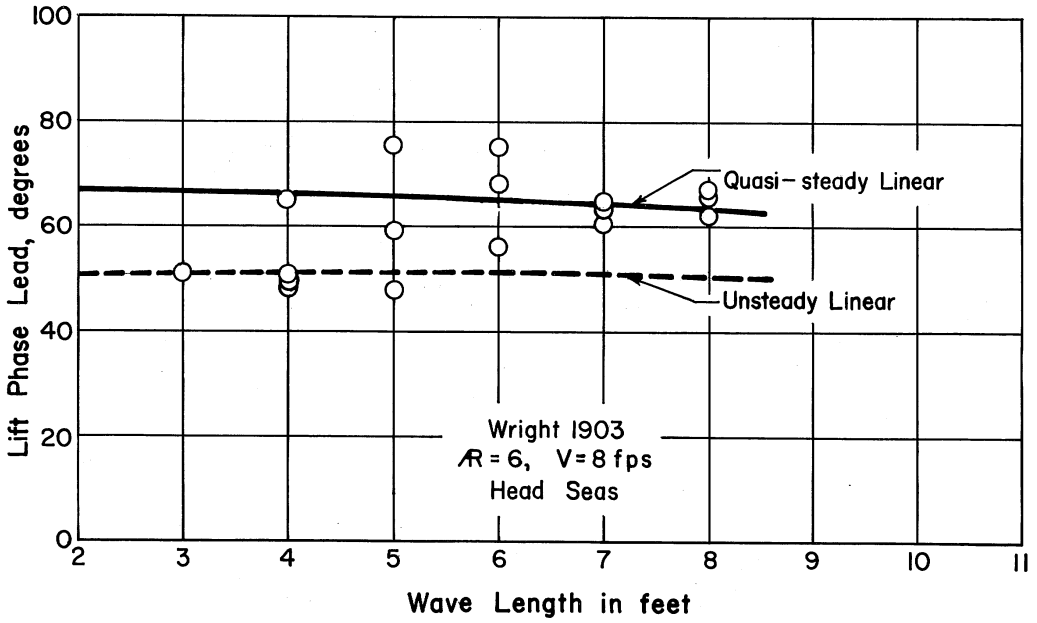

Fig. 6 – Oscillatory Lift Forces and Phase Relationships, Head Seas

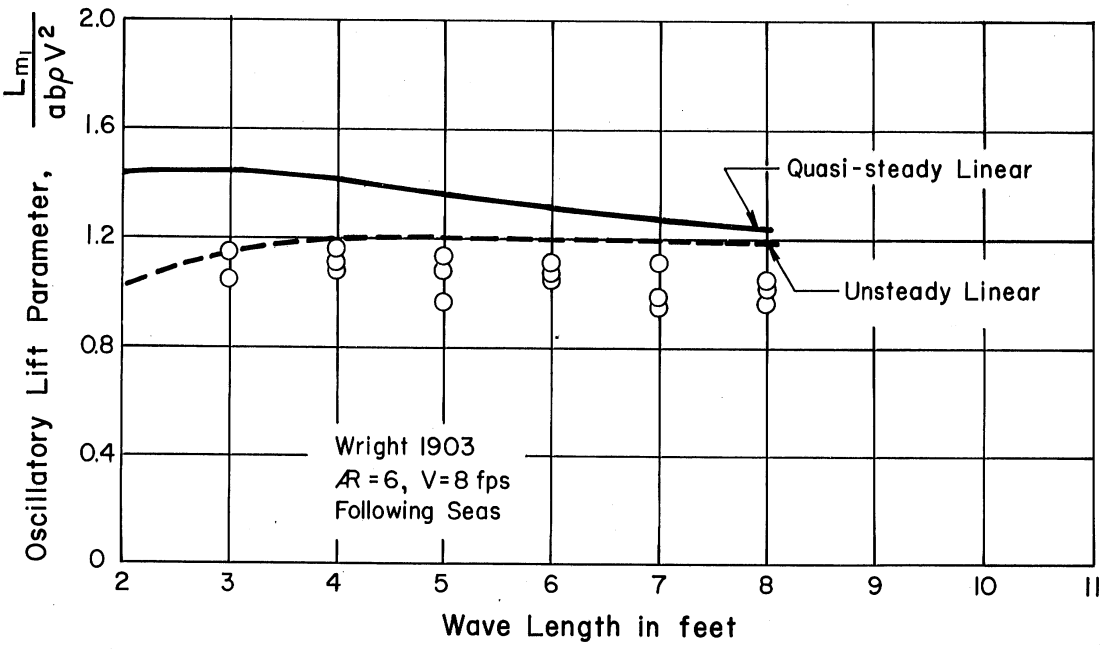

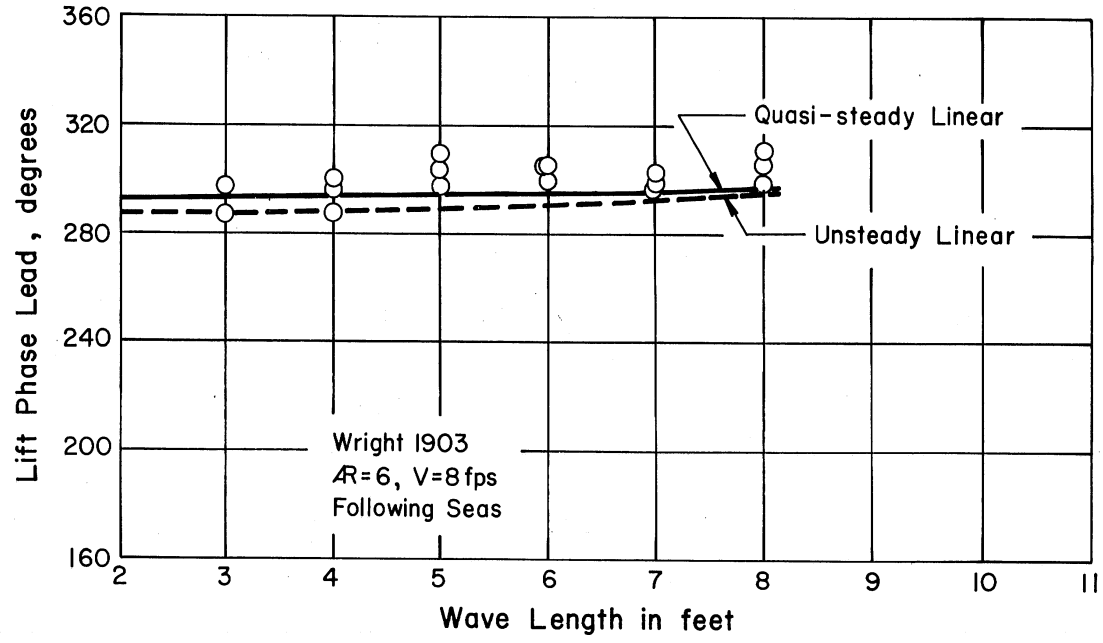

Fig. 7 – Oscillatory Lift Forces and Phase Relationships, Following Seas

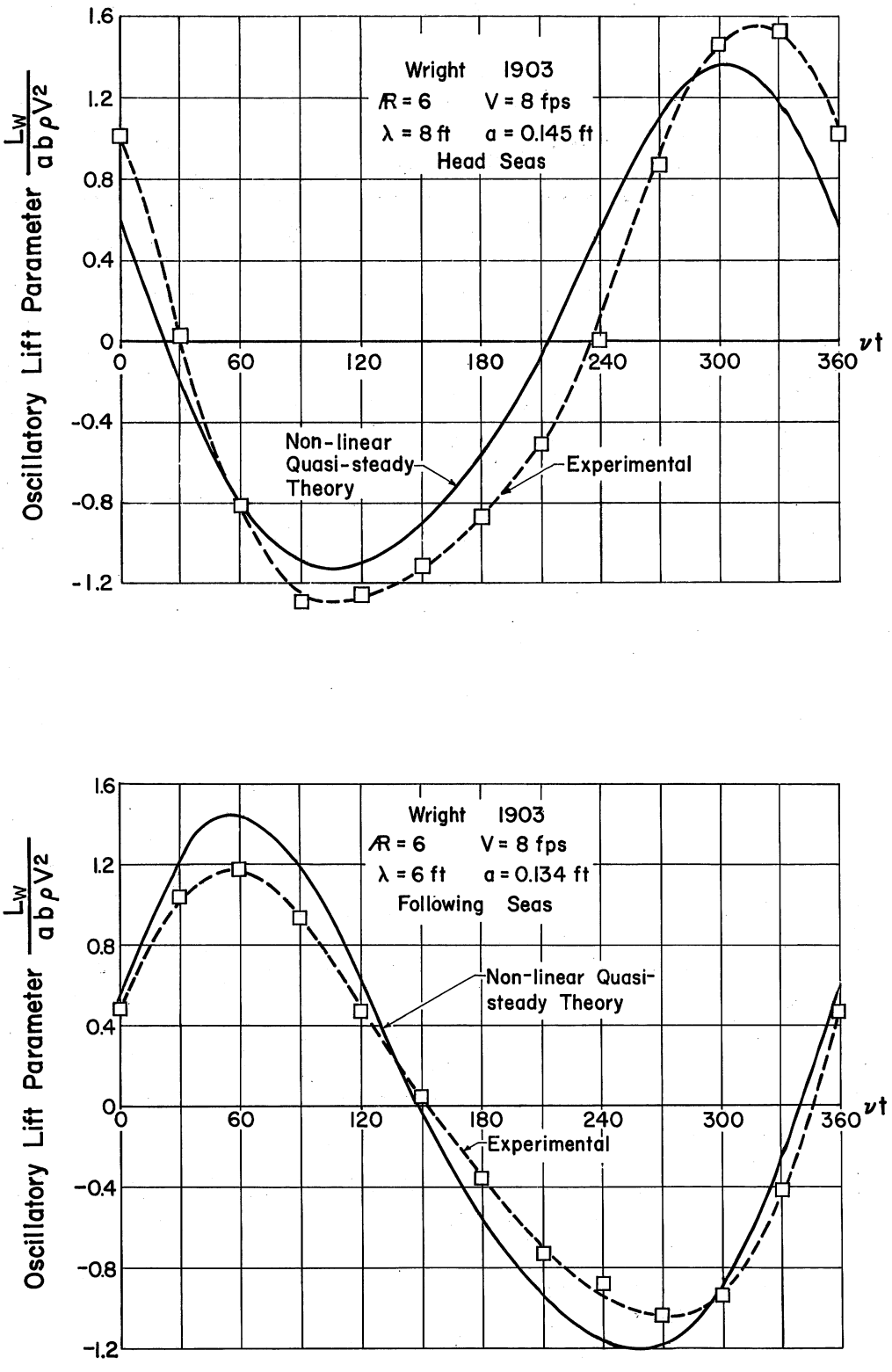

Fig. 8 – Comparison of Nonlinear Theory and Experimental Lift

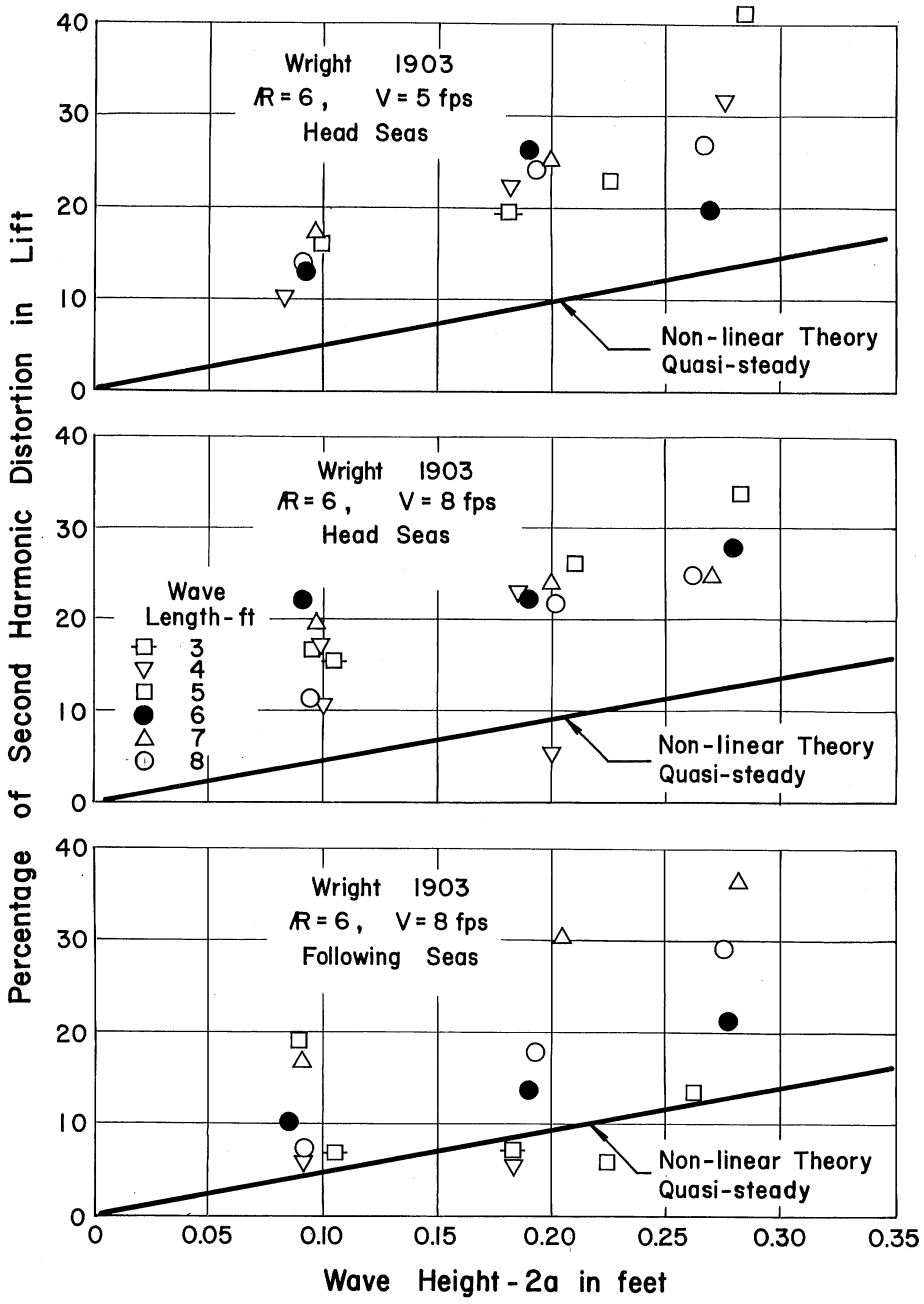

Fig. 9 – Percentage of Second Harmonic Distortion in Lift

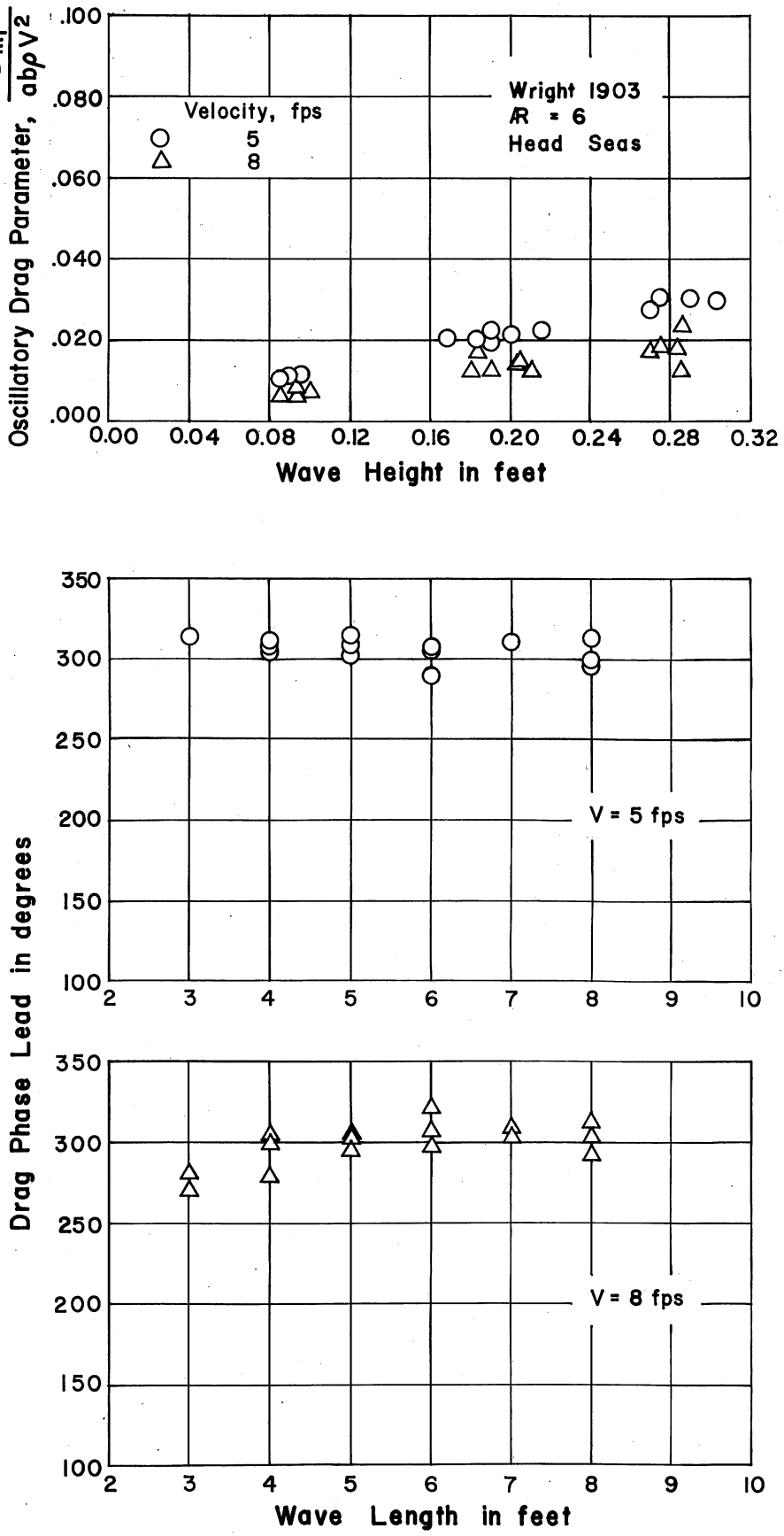

Fig. 10 – Oscillatory Drag Forces and Phase Relationships, Head Seas

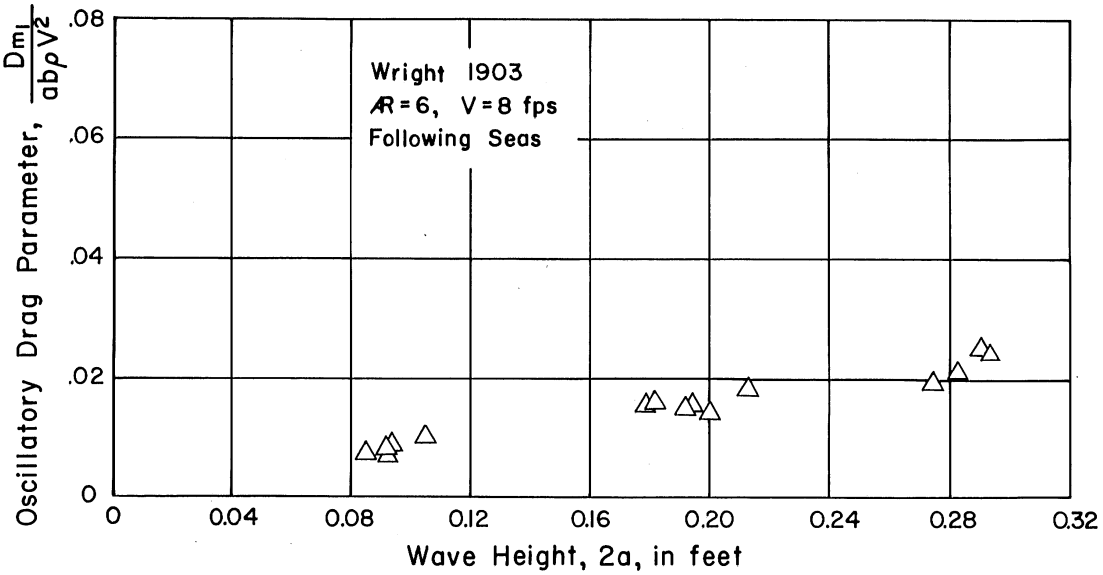

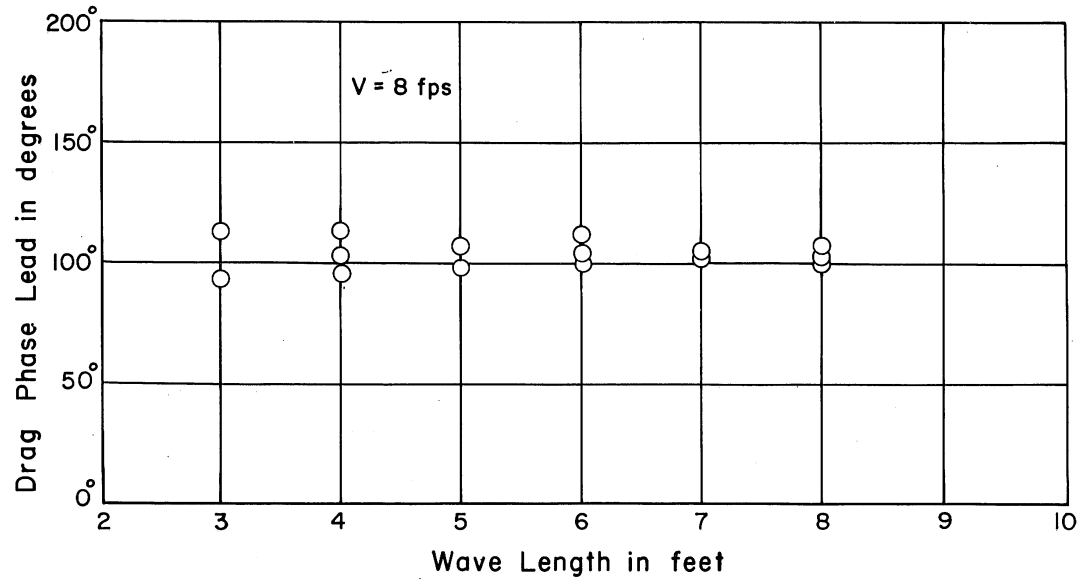

Fig. 11 - Oscillatory Drag Forces and Phase Relationships, Following Seas

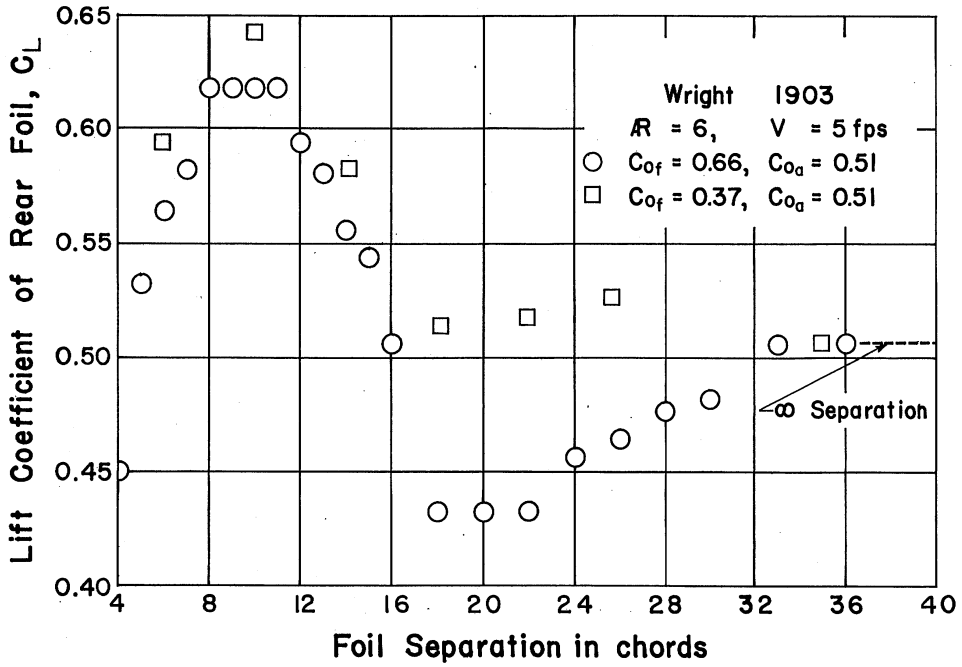

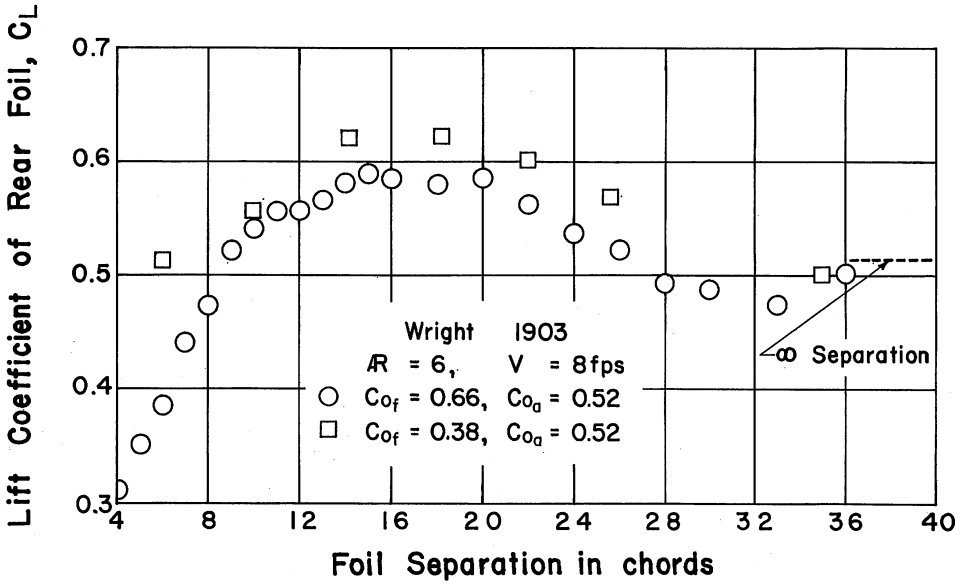

Fig. 12 – Lift Coefficients for Aft Foil of Tandem Configuration in Smooth Water

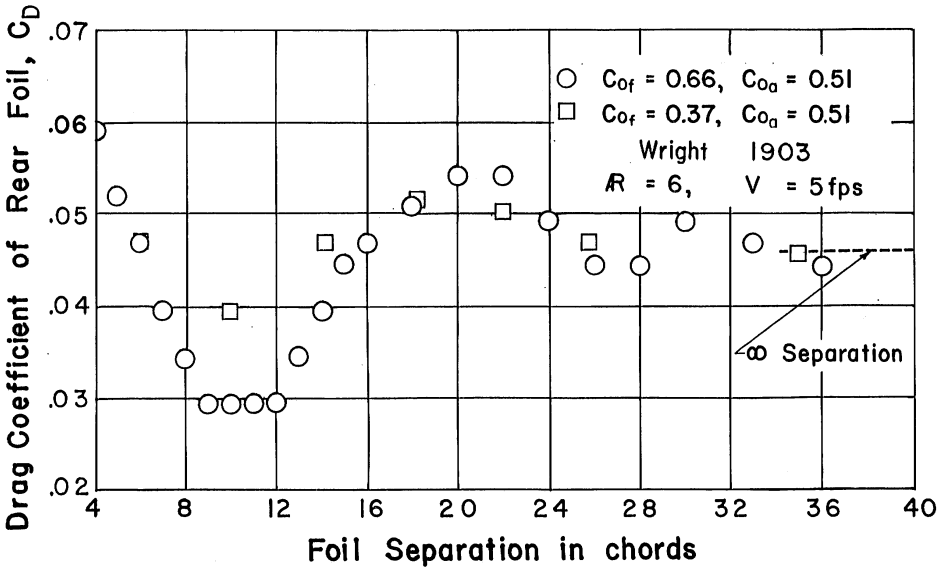

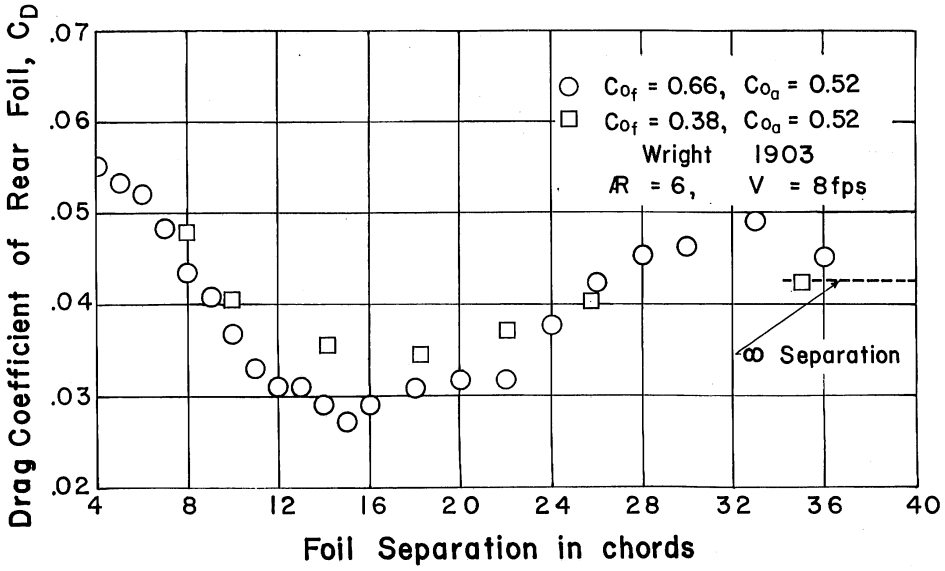

Fig. 13 - Drag Coefficients for Aft Foil of Tandem Configuration in Smooth Water

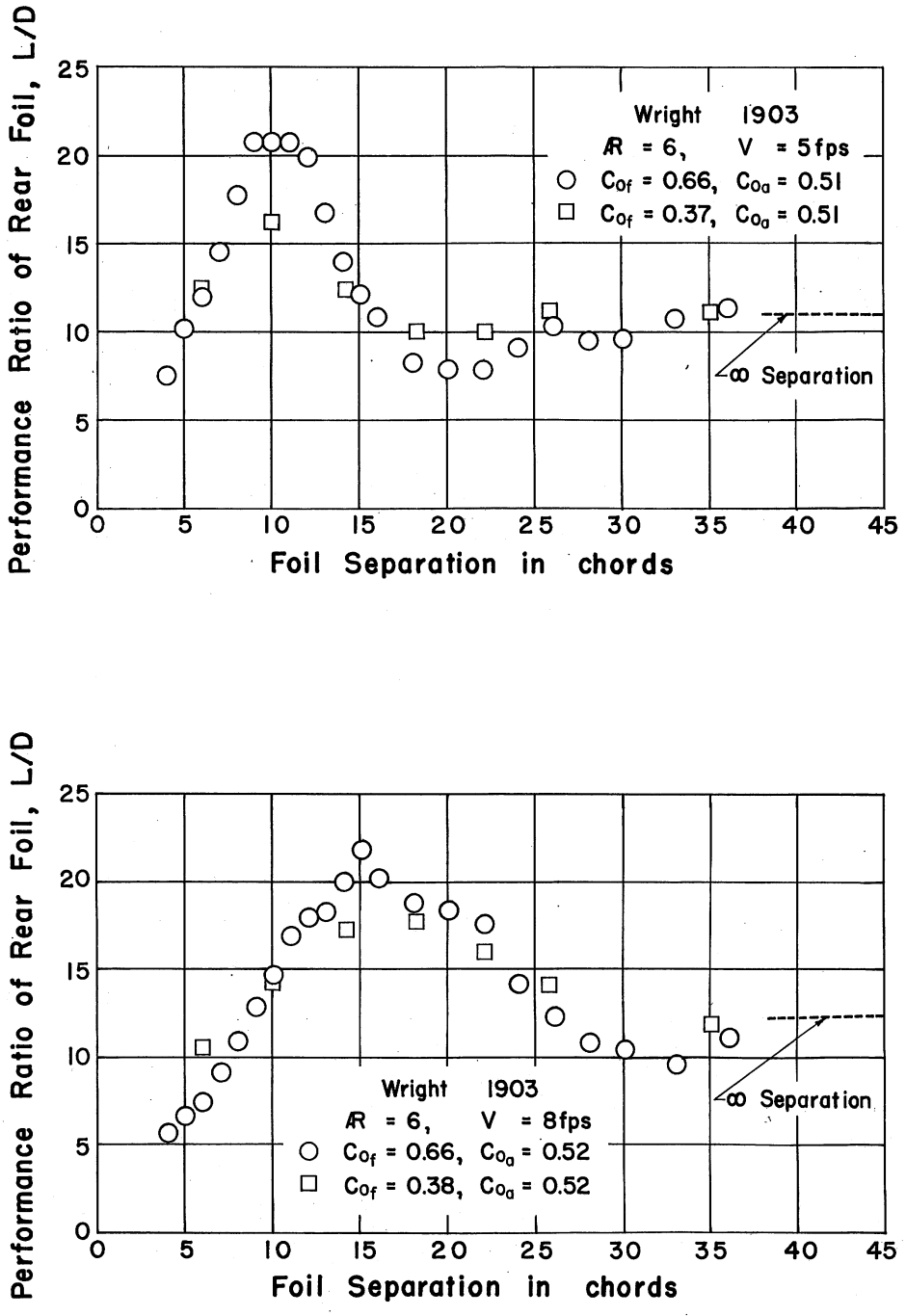

Fig. 14 - Performance Ratio for Aft Foil of Tandem Configuration

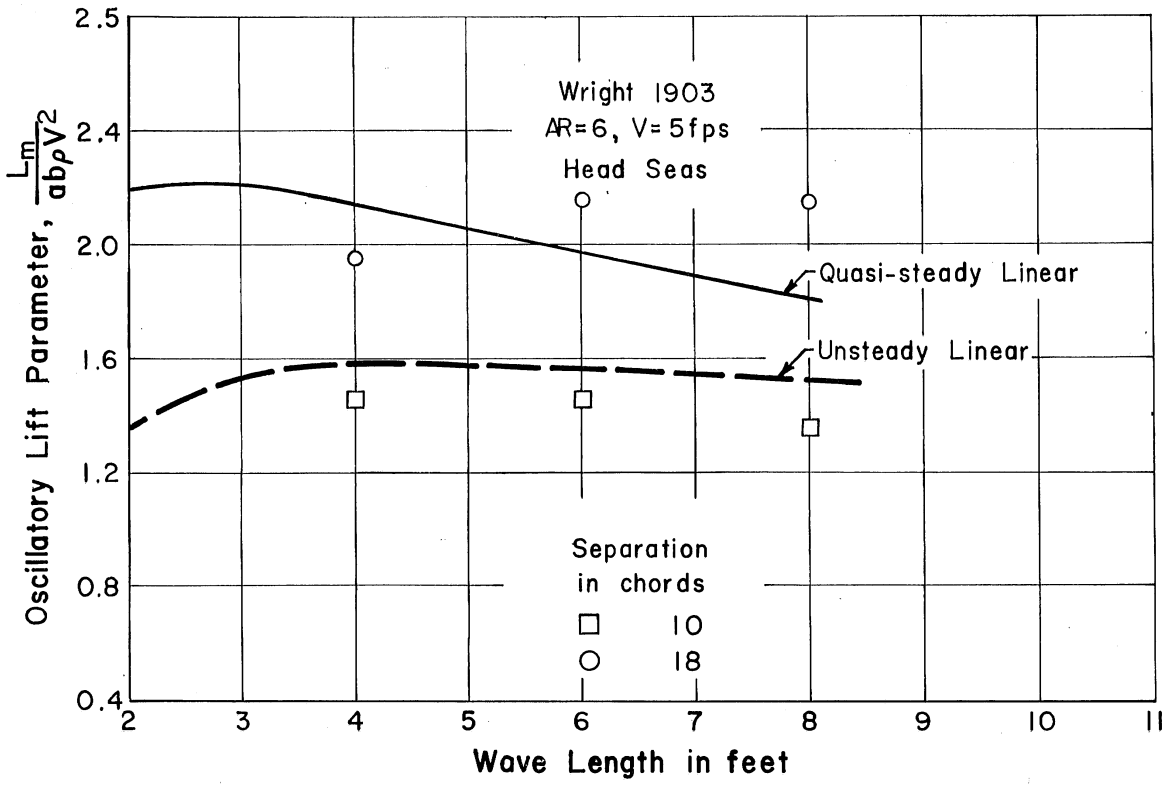

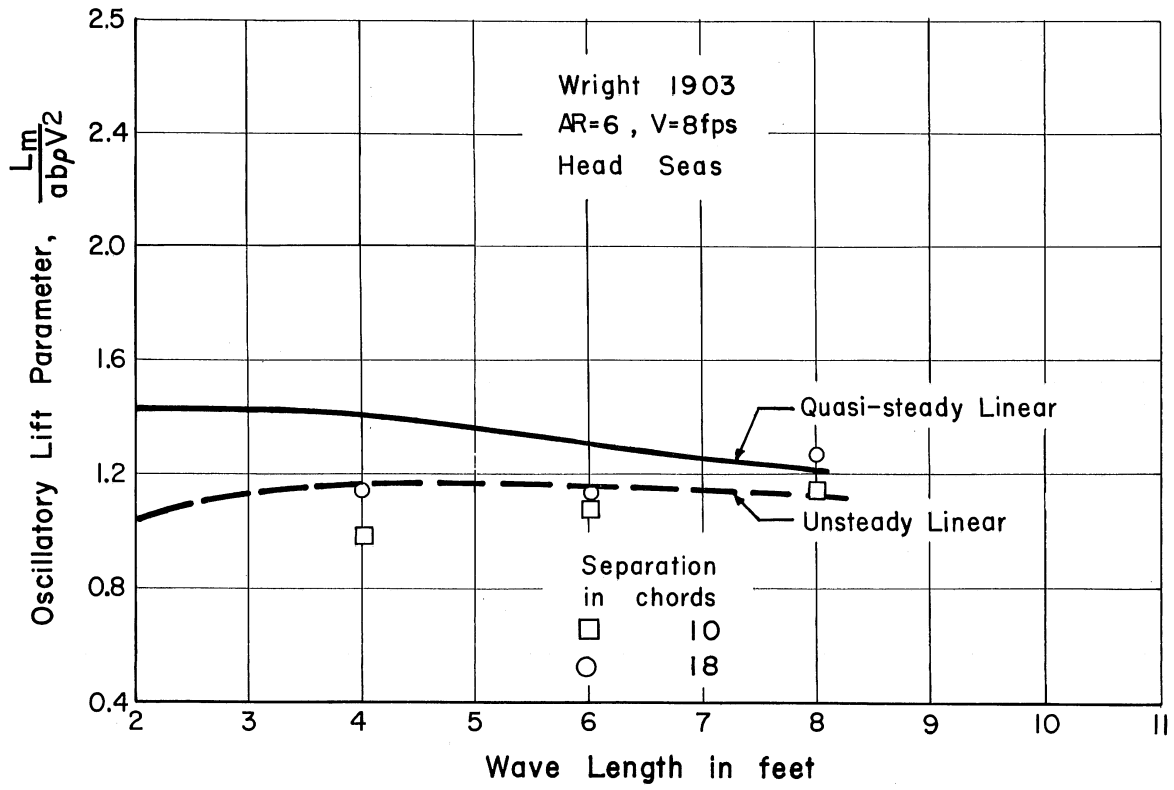

Fig. 15 – Oscillatory Lift Forces for Aft Foil of Tandem Configuration in Head Seas

A P P E N D I X

A P P E N D I X

Wright 1903
Chord = 2 in.
Aspect Ratio = 6
Dihedral Angle = 45°

Velocity = 5 fps Head Seas

Wave Length λ in ft	Wave Amplitude a in ft	L_{m_1} lbs	ϕ_{L_1} degrees	D_{m_1} lbs	ϕ_{L_1} degrees	Harmonic Components per cent Lift 2nd	Lift 3rd	Lift 4th	Drag 2nd	Drag 3rd	Drag 4th
3	0.091	1.31	60	0.08	315	19.95	7.89	7.45	31.8	13.8	5.6
4	0.042	0.73	61	0.04	310	10.35	3.22	2.14	13.6	11.5	8.19
4	0.091	1.29	63	0.08	310	22.7	1.93	0.76	45.3	12.25	21.9
4	0.138	1.97	76	0.12	312	31.8	9.89	6.22	45	9.36	8.83
5	0.050	0.65	69	0.05	304	16.32	1.37	4.53	30.2	7.22	2.92
5	0.113	1.4	72	0.09	310	23.05	11.47	5.61	45.6	13.75	4.13
5	0.142	2.24	73	0.12	316	41.3	6.39	2.59	60	19.1	4.55
6	0.046	0.71	63	0.05	291	13.77	6.46	4.9	39.6	5.22	5.51
6	0.095	1.41	58	0.08	309	26.7	1.77	9.11	49.6	12.58	5.41
6	0.135	2.19	64	0.13	306	20	7.16	2.33	44.6	5.87	2.1
7	0.046	0.86	69	-	-	17.7	8.45	5.34	-	-	-
7	0.100	1.55	67	0.09	312	25.3	7.2	5.62	51.7	19.17	11.56
8	0.047	0.79	69	0.04	298	14	12	5.53	22	10.55	1.35
8	0.097	1.67	77	0.09	314	24.2	8.98	5.52	28.4	12.87	6.41
8	0.134	2.15	67	0.11	301	27	8.34	3.94	44	18.08	13.54

Velocity = 8 fps Head Seas

3	0.053	1.44	51	0.07	272	15.6	1.9	1.2	21.2	4.7	4.1
4	0.050	1.24	48	0.06	279	17.15	3.86	5.49	14.8	4.49	3.34
4	0.050	1.13	50	-	-	10.73	5.54	4.97	-	-	-
4	0.093	2.31	65	0.18	302	23.2	9.88	6.81	32.2	26.7	20.43
4	0.100	2.52	49	0.19	304	5.3	6.65	5.38	46.3	12.06	6.06
5	0.048	0.85	47	0.08	297	16.7	8.6	6.06	15.8	6.64	6.8
5	0.105	2.67	59	0.13	305	26.6	4.21	1.05	36.9	8.59	10.16
5	0.142	4.11	76	0.24	303	33.75	9.78	3.13	39	7.7	3.28
6	0.046	1.55	76	0.08	298	22.6	6.65	1.8	38.3	5.61	5.3

Velocity = 8 fps Head Seas (conti.)

Wave Length λ in ft	Wave Amplitude a in ft	L_{m_1} lbs	ϕ_{L_1} degrees	D_{m_1} lbs	ϕ_{L_1} degrees	Harmonic Components per cent Lift 2nd	Lift 3rd	Lift 4th	Drag 2nd	Drag 3rd	Drag 4th
6	0.095	2.98	56	0.13	307	22.3	0.94	3.77	31	4.85	3.36
6	0.140	4.39	68	0.13	323	28.25	11.54	4.1	19.3	10.85	0.7
7	0.049	1.57	63	-	-	19.7	14.39	9.01	-	-	-
7	0.1	3.62	66	0.15	305	24.3	4.72	1.07	30.8	7.79	2.75
7	0.135	5.76	61	0.19	310	24.9	4.87	2.23	36	16.7	4.22
8	0.048	1.48	62	0.07	293	11.5	15.18	9.11	20.5	13.8	10.15
8	0.101	4.01	67	0.15	304	21.8	5.92	0.93	37.5	12.65	3.42
8	0.131	4.9	66	0.18	313	24.8	7.16	3.81	35.6	15.6	0.95
			Velocity = 8 fps		Following Seas						
3	0.053	1.26	287	0.34	94.2	6.95	11.7	4.7	15.4	7.44	3.68
3	0.091	1.97	297	0.32	113.2	7.26	2.22	7.68	30.3	9.33	10.64
4	0.046	0.1	296	0.32	104.4	6.19	7.15	2.4	17.2	13.54	7.02
4	0.092	2.21	300	0.32	114.3	6.95	5.75	9.83	27.5	11.36	1.45
4	0.131	3.02	288	0.29	96	13.35	1.65	7.23	24.3	11.59	4.21
5	0.05	0.89	264	0.32	99.8	40.98	3.03	5.49	10.8	3.01	7.96
5	0.078	3.25	310	-	-	4.35	5.77	4.92	-	-	-
5	0.112	2.62	319	0.31	107.1	6	6.071	3.88	27	8.23	9.02
6	0.043	0.94	310.8	0.32	100.1	10.4	5.6	1.58	14	1.25	3.92
6	0.098	1.11	180	0.33	112.8	13.8	3.42	0.51	30.8	11.2	4.61
6	0.139	3.1	320	0.29	105.5	21.3	3.53	0.18	28.8	10.94	9.33
7	0.046	0.95	299	-	-	17.1	3.16	1.77	-	-	-
7	0.103	2.37	299	0.28	105.6	20.9	10.49	5.1	21	4.14	7.16
7	0.141	2.87	303	0.29	103.5	36.5	12.86	9.92	30.7	7.96	7.91
8	0.046	0.99	306.5	0.38	102.9	7.41	3.04	3.49	24.48	6.11	7.9
8	0.097	2.1	310.5	0.29	101.7	17.8	7.2	3.81	18.9	7.86	5.66
8	0.138	2.77	299	0.33	109	29.2	22.67	14.62	20.9	11.12	2.15

NACA 0012
Chord = 2 in.
Aspect Ratio = 5
Dihedral Angle = 45°

Head Seas

Wave Length λ in ft	Wave Amplitude a in ft	Velocity fps	$\frac{L_m}{ab\,\rho\,V^2}$ Experimental	Quasi-Steady Calc.	Unsteady Calc.
3	0.10	5	1.19	0.92	0.63
	0.19		1.17		
	0.06	10	0.46	0.57	0.49
	0.10		0.65		
	0.18		0.76		
4	0.095	5	1.11	0.88	0.64
	0.195		1.14		
	0.285		1.26		
	0.095	10	0.62	0.56	0.49
	0.19		0.83		
	0.275		0.81		
5	0.09	5	1.17	0.85	0.63
	0.20		1.24		
	0.29		1.28		
	0.09	10	0.55	0.54	0.49
	0.20		0.81		
	0.285		0.74		
6	0.095	5	0.98	0.80	0.62
	0.195		1.21		
	0.285		1.26		
	0.085	10	0.44	0.52	0.49
	0.195		0.81		
	0.29		0.77		
7	0.095	5	1.04	0.77	0.62
	0.21		1.09		
	0.285		1.20		
	0.10	10	0.53	0.50	0.48
	0.21		0.74		
	0.285		0.78		

Head Seas (conti.)

Wave Length λ in ft	Wave Amplitude a in ft	Velocity fps	$\frac{L_m}{ab\,\rho\,V^2}$ Experimental	Quasi-Steady Calc.	Unsteady Calc.
8	0.10	5	0.99	0.73	0.60
	0.195		1.21		
	0.275		1.22		
	0.10	10	0.59	0.48	0.46
	0.20		0.77		
	0.285		0.74		
			Following Seas		
3	0.055	5	0.79		
	0.10		0.93		
	0.18		0.72		
	0.05	10	0.31	0.57	0.44
	0.09		0.22		
	0.182		0.49		
4	0.095	5	0.91		
	0.18		1.03		
	0.092	10	0.25	0.56	0.45
	0.18		0.53		
4	0.285	10	0.56		
5	0.10	10	0.28	0.54	0.45
	0.215		0.53		
	0.285		0.56		
6	0.10		0.23	0.52	0.45
	0.182		0.47		
	0.285		0.47		
7	0.10		0.23	0.49	0.45
	0.215		0.43		
	0.29		0.51		
8	0.10		0.23	0.47	0.44
	0.215		0.49		
	0.285		0.54		

SUGGESTED DISTRIBUTION LIST FOR PROJECT REPORT NO. 64
of the St. Anthony Falls Hydraulic Laboratory

Copies	Organization
65	Commanding Officer and Director, David Taylor Model Basin, Washington 7, D. C., Attn: Code 513.
5	Chief of Naval Research, Department of the Navy, Washington 25, D. C., Attn: Code 438 and 439.
3	Chief of Naval Operations, Department of the Navy, Washington 25, D. C., Attn: 1 - Code OP-31 1 - Code OP-07 1 - Code OP-34
1	Commanding Officer, Office of Naval Research, Branch Office, 346 Broadway, New York 13, New York.
1	Commanding Officer, Office of Naval Research, Branch Office, The John Crerar Library Building, 10th Floor, 86 East Randolph Street, Chicago 1, Illinois.
1	Mr. R. K. Johnston, Miami Shipbuilding Corporation, 615 S. W. Second Avenue, Miami 36, Florida.
1	Director, U. S. Naval Research Laboratory, Washington 25, D. C.
1	Commandant, U. S. Marine Corps, Department of the Navy, Washington 25, D. C., Attn: G-3.
1	Assistant Chief of Transportation for Military Operations, Department of the Army, Washington, D. C.
1	Director, Army Research Office, Department of the Army, Washington 25, D. C.
1	Secretary, Undersea Warfare Committee, National Research Council, 2101 Constitution Avenue, N. W., Washington, D. C.
1	Mr. J. G. Baker, President, Baker Manufacturing Company, Evansville, Wisconsin.
1	Dr. L. G. Straub, Director, St. Anthony Falls Hydraulic Laboratory, University of Minnesota, Minneapolis 14, Minnesota.
10	Chief, Bureau of Ships, Department of the Navy, Washington 25, D. C., Attn: 2 - Technical Information Branch (Code 335) 1 - Research and Development (Code 300) 1 - Noise Reduction Section (Code 345)

Copies	Organization
	1 - Preliminary Design (Code 420) 1 - Hull Design (Code 440) 1 - Scientific and Research (Code 442) 1 - Boats and Small Craft (Code 449) 1 - Mine, Service and Patrol Craft (Code 526) 1 - Landing Ships, Boats and Amphibious Vehicles (Code 529)
1	Chief, Bureau of Weapons, Department of the Navy, Washington 25, D. C., Attn: Code RRSY.
1	Commanding Officer, Office of Naval Research, Branch Office, 495 Summer Street, Boston 10, Massachusetts.
1	Commanding Officer, Office of Naval Research, Branch Office, 1030 East Green Street, Pasadena 1, California.
2	Commanding Officer, Office of Naval Research, Branch Office, Navy 100, F.P.O., New York, New York.
1	Director, National Aeronautics and Space Administration, 1512 H Street, N. W., Washington 25, D. C.
1	Commandant, U. S. Coast Guard, 1300 E Street, N. W., Washington 25, D. C.
1	Commandant, Marine Corps Schools, Quantico, Virginia, Attn: Marine Corps Development Center.
2	Director of Research and Development, Department of the Air Force, Washington 25, D. C.
1	Director, Weapons Systems Evaluation Group, Office of the Secretary of Defense, Washington 25, D. C.
1	Mr. T. M. Buerman, Gibbs and Cox, Incorporated, 21 West Street, New York 6, New York.
1	Commanding Officer, Office of Naval Research, Branch Office, 1000 Geary Street, San Francisco 9, California.
1	Professor H. A. Schade, Director, Institute of Engineering Research, Department of Engineering, University of California, Berkeley, California.
1	Dr. A. G. Strandhagen, Head, Department of Engineering Mechanics, University of Notre Dame, Notre Dame, Indiana.
1	Mr. W. R. Ryan, Edo Corporation, College Point 56, Long Island, New York.
1	Commander, Air Research and Development Command, P. O. Box 1395, Baltimore 3, Maryland, Attn: Rdtded.

Copies	Organization
10	Commander, Armed Services Technical Information Agency, Arlington Hall Station, Arlington 12, Virginia.
1	Mr. Philip Eisenberg, President, Hydronautics, Incorporated, 200 Monroe Street, Rockville, Maryland.
1	Officer in Charge, MWDP Contract Supervisory Staff, SACLANT ASW Research Center, APO 19, New York, New York.
1	Dr. R. C. Seamans, Radio Corporation of America, Waltham, Massachusetts.
1	Hydrodynamics Research Laboratory, Consolidated-Vultee Aircraft Corporation, San Diego 12, California.
1	Mr. J. D. Pierson, The Martin Company, Baltimore 3, Maryland.
1	Dynamic Developments, Incorporated, Seaplane Hangar, Midway Avenue, Babylon, Long Island, New York.
1	Dr. M. S. Plessett, Hydrodynamics Laboratory, California Institute of Technology, Pasadena, California.
1	Commanding Officer and Director, U. S. Naval Civil Engineering Laboratory, Port Hueneme, California, Attn: Code L54.
2	Dr. F. H. Todd, Director, National Physical Laboratory, Teddington, Middlesex, England (1 copy for Mr. A. Silverleaf).
1	Davidson Laboratory, Stevens Institute of Technology, Hoboken, New Jersey.
1	Technical Research Group, 2 Aerial Way, Syosset, L. I., New York, N. Y., Attn: Dr. Paul Kaplan.
1	Editor, Engineering Index, Inc., 29 West 39th Street, New York, N. Y.
1	Editor, Applied Mechanics Reviews, Southwest Research Institute, 8500 Culebra Road, San Antonio 6, Texas.
1	Librarian, Institute of Aerospace Sciences, 2 East 64th Street, New York 21, N. Y.
1	Librarian, Society of Naval Architects and Marine Engineers, 74 Trinity Place, New York 6, N. Y.
1	Chief, Office of Research and Development, Maritime Administration, U. S. Department of Commerce, Washington 25, D. C.